RSC Advances

PAPER

View Article Online
View Journal | View Issue

Cite this: *RSC Adv.*, 2020, **10**, 18740

Adsorptive, kinetics and regeneration studies of fluoride removal from water using zirconium-based metal organic frameworks

Tong Ling Tan, *[a] Poovarasi A/P Krusnamurthy,[b] Hideki Nakajima[c] and Suraya Abdul Rashid*[ab]

Fluoride contamination has been recognised as one of the major problems worldwide, imposing a serious threat to human health and affecting the safety of drinking water. Adsorption is one of the widely considered appropriate technologies for water defluorination. The present study describes the preparation of a zirconium-based metal organic framework (MOF-801) adsorbent using a solvothermal method and its adsorption efficiency for removal of fluoride ions from water. The morphology of MOF-801 was characterized by PXRD, FESEM and XPS, and the pore structure and surface area were calculated according to BET. It was found that the synthesized MOF-801 showed the distinguishable octahedral shape particle with a lattice spacing of 0.304 nm, indicative of (011) planes of ZrO_2. Adsorption studies were carried out to study the defluorination effectiveness by varying contact time (30–150 min), adsorbent dose (0.3–1.5 g L^{-1}), adsorbate concentration (5–25 mg L^{-1}), as well as kinetics and isotherms. The maximum removal efficiency for fluoride using MOF-801 at equilibrium was found to be 92.3%. Moreover, the adsorption kinetic studies indicate that the overall fluoride adsorption process was best described by pseudo-second-order kinetics. The adsorption data were well-fitted with the Langmuir isotherm model (R^2 = 0.9925) with maximum adsorption capacity of 19.42 mg g^{-1}. The synthesized MOF-801 had good reusability and was used in up to four cycles for fluoride removal attaining around 79% removal efficiency after the fourth cycle. All the results suggested that the synthesized MOF-801 has potential to be an excellent adsorbent for wastewater defluorination treatment.

Received 10th February 2020
Accepted 2nd May 2020

DOI: 10.1039/d0ra01268h

rsc.li/rsc-advances

1. Introduction

Fluoride, a natural element which is usually present in various water bodies, can have beneficial as well as detrimental effects on humans depending on its concentration and the total amount ingested. Fluoride contamination in groundwater has become a worldwide environmental issue which is caused both by natural geological processes and industrial sources. It is considered an essential micronutrient for human health in facilitating the mineralization of bone and preventing dental caries if consumed at a recommended range of concentration. According to the World Health Organization (WHO), the permissible limit of fluoride concentration in drinking water is generally 1.5 mg L^{-1}.[1–5] In contrast, it is noted that the long-term intake of higher quantities of fluoride will pose adverse health effects to humans, leading to a variety of diseases including skeletal fluorosis, osteoporosis, arthritis, brittle bones, cancer, infertility, thyroid disorder, and even interference with DNA synthesis.[6–10]

Fluorosis, associated with elevated fluoride concentrations in drinking water, has been reported in various countries around the world such as India, China, Tanzania, Mexico, Argentina, and South Africa.[8] Dental fluorosis occurs in 10% of children exposed to 4 mg L^{-1} fluoride in their drinking water, where skeletal fluorosis occur when the fluoride concentration is greater than 10 mg L^{-1}.[9] Furthermore, a study published in Environmental Health Perspectives in 2012 found that a high level of fluoride in drinking water has potential in lowering IQ levels in children.[6,10] In Malaysia, the recommended level of fluoride in the public water supply is 0.4 to 0.6 mg L^{-1}. However, it was found that 7% of the population in Malaysia are exposed to a public water supply which exceeded the upper limit of the recommended fluoride level which is more than 0.6 ppm.[3,4] Considering the view of the toxic effects of fluoride on human health, it is imperative to propose an effective and robust technology to mitigate the excess fluoride from drinking water to the permissible limit from the perspective of environmental sustainability and public health.

[a]*Institute of Advanced Technology, Universiti Putra Malaysia, 43400 UPM Serdang, Selangor, Malaysia. E-mail: suraya_ar@upm.edu.my; tongling@upm.edu.my*
[b]*Department of Chemical and Environmental Engineering, Faculty of Engineering, Universiti Putra Malaysia, 43400 UPM Serdang, Selangor, Malaysia*
[c]*Synchrotron Light Research Institute (Public Organization), 111 Moo 6 University Avenue, Muang District, Nakhon Ratchasima 30000, Thailand*

To date, numerous methods have been developed for fluoride removal from water such as ion exchange, membrane process, electrodialysis, precipitation and coagulation.[11,12] However, the shortcomings of most of these methods are high maintenance and operational costs, secondary pollution (toxic sludge being created), and complicated steps.[13,14] Among the various techniques available, adsorption method seems to be superior because of its flexibility, cost effectiveness, environmentally friendly, simple design and easy operation.[15] Different adsorbents have been reported for the removal of fluoride, including activated alumina, carbonaceous materials, activated clay, rare earth oxides, titanium rich bauxite, zeolites and biomaterials. The most commonly used adsorbent for fluoride removal is activated alumina (AA) but with a few drawbacks such as relatively high cost, difficulties in regeneration and disposal of the exhausted adsorbent.[16,17] Therefore, developing an effective adsorbent with high adsorptive capacity and low production cost for defluorination still remains a challenge and warrants further exploration.

Metal Organic Frameworks (MOF), as a new class of three-dimensional crystalline inorganic–organic porous hybrid materials with tunable pore architectures and exceptional internal surface area, have emerged as a promising candidates for a wide range of applications including gas storage, catalysis, ion exchange, sensor, drug delivery as well as adsorption and removal of hazardous materials.[17,18] MOF have been widely exploited for the adsorption of contaminant-related applications due to their high surface area, rich surface functional groups, highly ordered atomic arrangement as well as controllable pore size and shape for facilitating the uptake of targeted compounds.[19,20] In recent years, the research on the removal and adsorption of pollutants from aqueous environment by MOF has attracted considerable attention. Chen *et al.* synthesized Zr-metal organic framework, UiO-66, which provided valuable insights into the development of efficient MOF-based adsorbents for the adsorption of anticonvulsant carbamazepine and tetracycline hydrochloride.[21] Nguyen *et al.* prepared MOF MIL-53(Fe) (MIL = Materials of Institute Lavoisier) using a solvothermal method with 80% adsorption of ibuprofen from water.[22] Chen *et al.*, reported DUT (Dresden University of Technology)-67 (Zr) MOF with large specific surface area of 781.8 $m^2\ g^{-1}$ for removing trace mercury (90%) and methylmercury ions (77%) respectively in water.[23] The obtained results demostrated the potential of MOF for rapid and efficient removal of pollutants from aqueous solutions.

Among all of these MOF, zirconium-based MOF (Zr-MOF) have demonstrated higher adsorption capacity and are thermally and chemically stable in fluoride solution.[24] MOF-801 is the smallest member of Zr-MOF with a formula of $(Zr_6O_4(OH)_4(fumarate)_6 \cdot xH_2O)$. It is constructed from $ZrCl_4$ and fumaric acid; possess good water stability, large surface area, and UiO-66 type network topology, which have made MOF-801 to be a good adsorbent for the removal of fluoride from water.[25] The presence of zirconium-bound hydroxyl groups in the nodes of MOF-801's framework facilitates fluoride adsorption by anion-exchange behaviour. In the present study, MOF-801 was synthesized by the solvothermal method and its removal efficiency of fluoride from water was investigated. Batch sorption experiments including adsorption kinetics and isotherms were carried out. The factors that affected adsorption performance including contact time, adsorbent dosage and fluorine concentration were studied in detail and the regeneration studies of MOF-801 was also investigated.

2. Experimental

2.1 Materials

The chemical substances used for the synthesis of MOF-801 were fumaric acid, $C_4H_4O_4$ (99% Sigma-Aldrich), zirconyl chloride octahydrate, $ZrOCl_2 \cdot 8H_2O$ (98%, Sigma-Aldrich), dimethylformamide (DMF), C_3H_7NO (Emsure), methanol, CH_3OH (R&M Chemicals) and formic acid, CH_2O_2 (Emsure). The chemical substance used for the adsorption of fluoride was sodium fluoride, (NaF) powder (R&M Chemicals). Sodium hydroxide, NaOH (QReC) pellets was used for the regeneration of MOF-801. DI water was used throughout the experiments.

2.2 Synthesis of MOF-801

MOF-801 was successfully synthesized using a solvothermal technique. In a 100 mL Schott Durran bottle, 1.16 g of fumaric acid ($C_4H_4O_4$) and 3.2 g of zirconyl chloride octahydrate ($ZrOCl_2 \cdot 8H_2O$) were dissolved in a mixed solvent of 40 mL of DMF and 14 mL of formic acid. The mixture was then heated in an isothermal oven at 130 °C for 6 hours to give as-prepared MOF-801 as white precipitate. After cooling to room temperature, the mixture was centrifuged at 10 000 rpm and washed with DMF and methanol for removing residual reactants. Then, the while solid precipitate obtained was dried at 80 °C for 24 h, yielding activated MOF-801 as a white powder. A schematic diagram for the preparation of MOF-801 and synthesis mechanism was shown in Fig. 1. MOF-801 is formed by the regular arrangements of organic linkers and inorganic metal ions.

2.3 Materials characterization

The structure of the synthesized MOF-801 was confirmed by Particle X-ray Diffraction (PXRD, X'Pert Pro PANalytical, PW 3040/60). PXRD analysis was performed at 25 °C and at scan step time and size of 8.06 s and 0.0170°. The diffraction patterns were recorded using CuKα radiation in the range of 2θ from 5° to 50°. The porous structure of synthesized MOF-801 was studied by low temperature N_2 adsorption at 77 K on a micromeritics Tristar II Plus adsorption analyser. The samples were degassed at 150 °C for 3 h before N_2 adsorption measurement. The specific surface area was calculated using Brunauer, Emmett and Teller (BET) analysis of the adsorption branch of the isotherm in the relative pressure range of 0.01–0.02. The total pore volume was calculated from the amount of N_2 adsorbed at a relative pressure $P/P_0 = 0.99$. The morphology of the MOF-801 was performed by Field Emission Scanning Electron Microscope (FESEM, NOVA NANOSEM 230) and using High Resolution Transmission Electron Microscope, HRTEM (FEI-Tecnai F20). The surface chemical compositions of the MOF-801 was detected by X-ray photoelectron spectroscopy (XPS) using Synchrotron Light Research Institute (SLRI) Thailand.

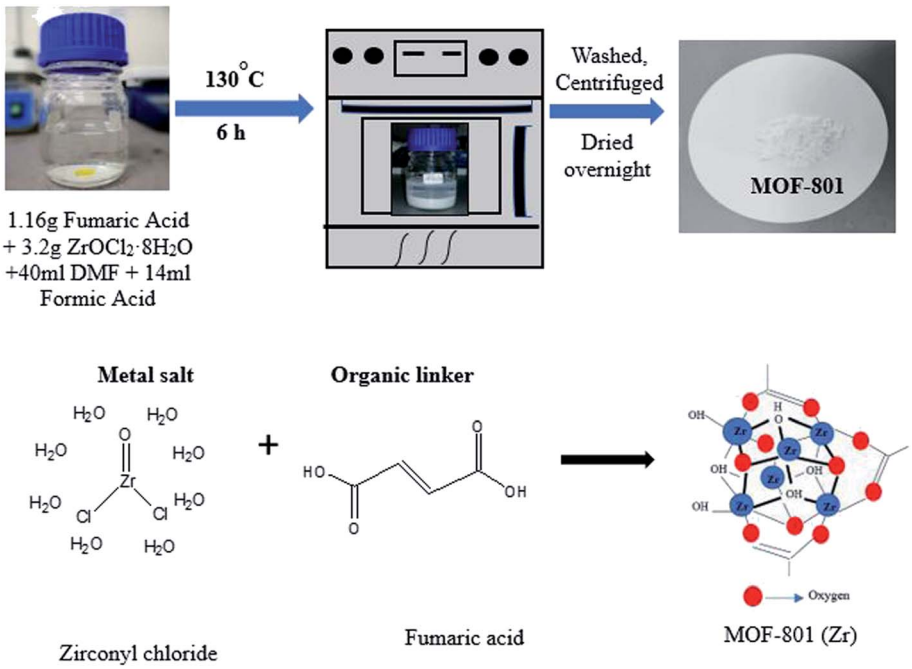

Fig. 1 Schematic diagram of MOF-801 synthesis and formation mechanism.

2.4 Batch adsorption test

In batch adsorption experiments, a fluoride stock solution with a concentration of 25 mg L^{-1} was prepared by dissolving NaF in DI water, and diluted to the expected concentrations (5, 10, 15, 20 and 25 mg L^{-1}) for the subsequent adsorption experiments. Then, a certain amount of the MOF-801 adsorbent (0.3 g L^{-1}, 0.6 g L^{-1}, 0.9 g L^{-1}, 1.2 g L^{-1} and 1.5 g L^{-1}) was added to the conical flask and the mixture was shaken in an incubator shaker (Heidolph Unimax 1010) at a speed of 200 rpm for a predetermined contact time (30, 60, 90, 120 and 150 min). The adsorption of fluoride on MOF-801 was evaluated using these three parameters (contact time, fluoride initial concentration and amount of MOF-801) to identify the optimum condition for maximum uptake of fluoride removal from water. All the experiments were performed in triplicates at room temperature (25 °C) and average data were taken to evaluate performance. For each sample, 6 mL of sample solution was collected and filtered using 0.22 μm nylon membrane to separate the fluoride containing MOF-801 from the sample solution. The filtered supernatant was then analysed using ion chromatography to determine the fluoride concentration present in it. This equipment provides high sensitivity and selectivity for the determination of inorganic anions such as fluoride. Finally, the removal efficiency of fluoride was calculated according to eqn (1).

$$\text{Removal efficiency} = ((C_0 - C_e)/C_0) \times 100 \quad (1)$$

where C_0 and C_e refer to the initial and equilibrium concentration of fluoride (mg L^{-1}), respectively.

The equilibrium adsorption capacity, q_e was calculated from eqn (2):

$$q_e = \left(\frac{(C_0 - C_e)}{m} \times V\right) \quad (2)$$

where C_0 and C_e refer to the initial and equilibrium concentration of fluoride (mg L^{-1}), respectively, V the volume of fluoride solution (L), and m is the mass of MOF-801 (g).

2.5 Adsorption kinetics and isotherm studies

The results obtained from the effect of contact time and initial fluoride concentration was further analysed to deepen the understanding on fluoride adsorption behaviour of MOF-801 using adsorption kinetics models (pseudo-first order and pseudo-second order models) and adsorption isotherms (Langmuir and Freundlich isotherms). Adsorption kinetics is used to study the rate of fluoride adsorption on MOF-801. Pseudo-first order and pseudo-second order models were applied to utilize the present adsorption data to determine the related adsorption kinetics parameter. The linear equations of pseudo-first-order model and pseudo-second-order model are as shown in eqn (3) and (4).

$$\ln(q_e - q_t) = \ln q_e - (k_{1t})/2.303 \quad (3)$$

$$t/q_t = 1/(k_2 q_e^2) + t/q_e \quad (4)$$

where q_e is the amount of fluoride adsorbed per unit weight of MOF-801 at equilibrium (mg g^{-1}), q_t is the amount of fluoride adsorbed per unit weight of MOF-801 (mg g^{-1}) at time t (min) and k_1 and k_2 is the first and second order rate constant for the adsorption (min^{-1}) respectively. In the kinetic tests, 1 g L^{-1} of MOF-801 was immersed into 10 mg L^{-1} of fluoride solution, and each 6 mL sample was collected at different time intervals (30–150 min) for fluoride analysis.

Adsorption isotherm was used to describe the relationship between the amount of fluoride adsorbed on the surface of MOF-801 and its equilibrium concentration in the solution at constant temperature and pressure. The adsorption isotherms were evaluated with initial fluoride concentrations set between 5 and 25 mg L^{-1}. The experimental results were modelled using Langmuir and Freundlich isotherm models to obtain the best fitting model.

The linear form of Langmuir isothermal model is shown in eqn (5):

$$C_e/q_e = 1/(q_m K_L) + (1/q_m)C_e \quad (5)$$

where C_e is the equilibrium concentration of fluoride in the solution (mg L^{-1}); q_e is the amount of fluoride adsorbed per unit weight of MOF-801 (mg g^{-1}), q_m is the maximum adsorption capacity (mg g^{-1}) and K_L is the Langmuir constant related to energy (L mg^{-1}).

The linear form of Freundlich equation is shown in eqn (6).

$$\ln q_e = \ln K_F + \ln C_e/n \quad (6)$$

where C_e is the equilibrium concentration of fluoride in the solution (mg L^{-1}); q_e is the amount of fluoride adsorbed per unit weight of MOF-801 (mg g^{-1}), K_F and n are dimensionless constants which are relative adsorption capacity and intensity of adsorption respectively.

The residual fluoride concentration was determined by an ion chromatographic separation (881 Compact IC plus ion chromatography) with 2 mM sodium carbonate (Na_2CO_3) and 0.8 mM sodium bicarbonate ($NaHCO_3$) as eluent with a flow rate of 0.7 mL min^{-1}.

2.6 Regeneration of MOF-801

Desorption of MOF-801 was performed by using 0.1 M sodium hydroxide (NaOH) as the regenerant. The fluoride saturated MOF-801 was suspended in 40 mL of 0.1 M NaOH solution and shake using shaker at 200 rpm for 6 hours for desorption of fluoride by MOF-801. MOF-801 was then separated from the NaOH solution by using 0.22 μm nylon membrane filter. The filtered MOF-801 was then heated in oven at 80 °C for 5 hours to be reused for the adsorption of fluoride from aqueous solution. After each run, the fluoride concentration of the filtrate was determined by ion chromatographic separation. Following the above procedure, the recycled MOF-801 was reused up to four times.

3. Results and discussion

3.1 Characterization of MOF-801

The as-synthesized MOF-801 was characterized by PXRD, XPS, FESEM and N_2 adsorption analysis. The phase purity of the samples was checked by PXRD. Fig. 2a shows the PXRD pattern of the as-synthesized of MOF-801. For comparison, the pattern of simulated MOF-801 from the crystallographic data is also included. As shown in Fig. 2a, all of the experimental PXRD pattern diffraction peaks are well matched with the simulated pattern in previous literature.[24,26] The main diffractions peaks at 8.66°, 9.97° and 25.90° were found to be in agreement with the (111), (002) and (244) facet of Zr-MOF.[27] Additionally, the peak intensity obtained was high, indicating high crystallinity and no miscellaneous PXRD peaks were observed, suggesting the successfully synthesis of MOF-801. The high crystallinity property of MOF-801 was also supported by the FESEM image of the material (Fig. 2b and c). FESEM revealed that the as-synthesized MOF-801 were of octahedron shaped morphology with relatively uniform size and good dispersity. TEM was further used to identify the morphology of MOF-801 nanoparticles (Fig. 2d and e). We could observe that the MOF-801 exhibited a narrow size distribution, which are in good agreement with the FESEM observation. The magnified TEM image of MOF-801 exhibit dense and well-defined octahedral morphology. Moreover, high resolution transmission electron microscopy (HRTEM) image from Fig. 2f shows a lattice fringe spacing of 0.304 nm which corresponds to the (011) planes of ZrO_2.[28] The average particle size of the MOF-801 obtained using software ImageJ (random 50 particles) was 269.4 ± 2.97 nm.

XPS was employed to investigate the chemical compositions, especially the valence state of the elements in MOF-801. The XPS wide scan, as presented in Fig. 3a, confirms that the existence of C, O, and Zr in the MOF-801 sample. The high-resolution of Zr 3d spectrum is shown in Fig. 3b, the Zr 3d peaks appeared at binding energies of 182.89 and 185.21 eV, referring to $3d_{5/2}$ and $3d_{3/2}$ of Zr(IV), which matched with reported Zr-based MOFs.[24,25] The O 1s spectra of MOF-801 as shown in Fig. 3c, can be represented by two peaks, zirconium oxide bond (Zr–O, at around 530.2 eV) and zirconium hydroxyl bond (Zr–OH, at around 531.7 eV).[25] Nitrogen adsorption–desorption isotherms were analysed to determine the surface area and pore structures of MOF-801 and the results are displayed in Fig. 3d. The N_2 adsorption–desorption isotherm of MOF-801 constitutes typical type-I curves, which is characteristic of typical microporous materials and the adsorption on MOF-801 is based on monolayer adsorption. The Brunauer–Emmett–Teller (BET) surface area is 522 m^2 g^{-1}, and the calculated pore volume is found to be 0.26 cm^3 g^{-1}. Pore size distribution calculated from the desorption isotherm using the Barrett–Joyner–Halenda (BJH) method as shown in Fig. 3e indicates the presence of micropores with an average pore diameter of 1.51 nm. The high surface area and microporous morphology are likely to benefit the adsorption performance.

3.2 Adsorption studies for fluoride

3.2.1 Effect of contact time. Since contact time is a crucial parameter for the evaluation of the performance of the adsorbent, the time required for adsorbents to reach adsorption equilibrium was determined. To investigate the effect of the contact time, adsorption experiments were performed from 30 to 150 min at initial fluoride concentration of 10 mg L^{-1}. As shown in Fig. 4a, the fluoride was adsorbed rapidly at the initial stage (t < 30 min), then continued to be adsorbed at a relatively slower rate. During the first 30 min, higher amounts of fluoride were removed as the fluoride ions bind to the readily available

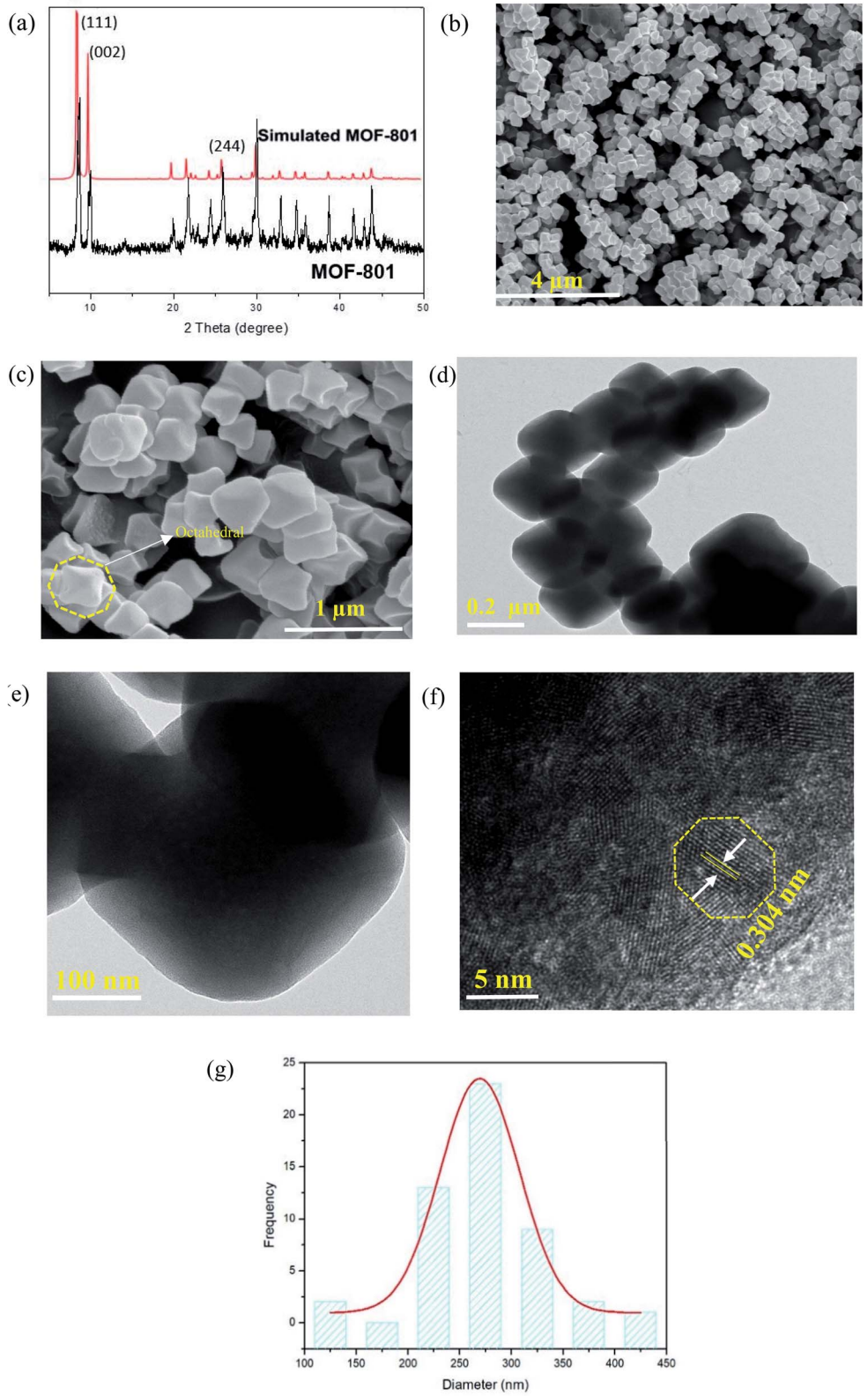

Fig. 2 (a) PXRD of MOF-801, FESEM of MOF-801 at (b) low magnification (25k×); (c) high magnification (100k×), TEM of MOF-801 at (d) low magnification (2.3k×); (e) high magnification (8.9k×), (f) HRTEM of MOF 801 and (g) particle size distribution of MOF-801.

active sites on the outer surface of MOF-801 instantaneously. The slower uptake of fluoride after 30 minutes is due to gradual diffusion of fluoride ions into the interior surface of the porous MOF-801.[25] The sorption process for fluoride ion was observed even in small span of time due to fast initial stage adsorption which was followed by a second stage with a relatively slow

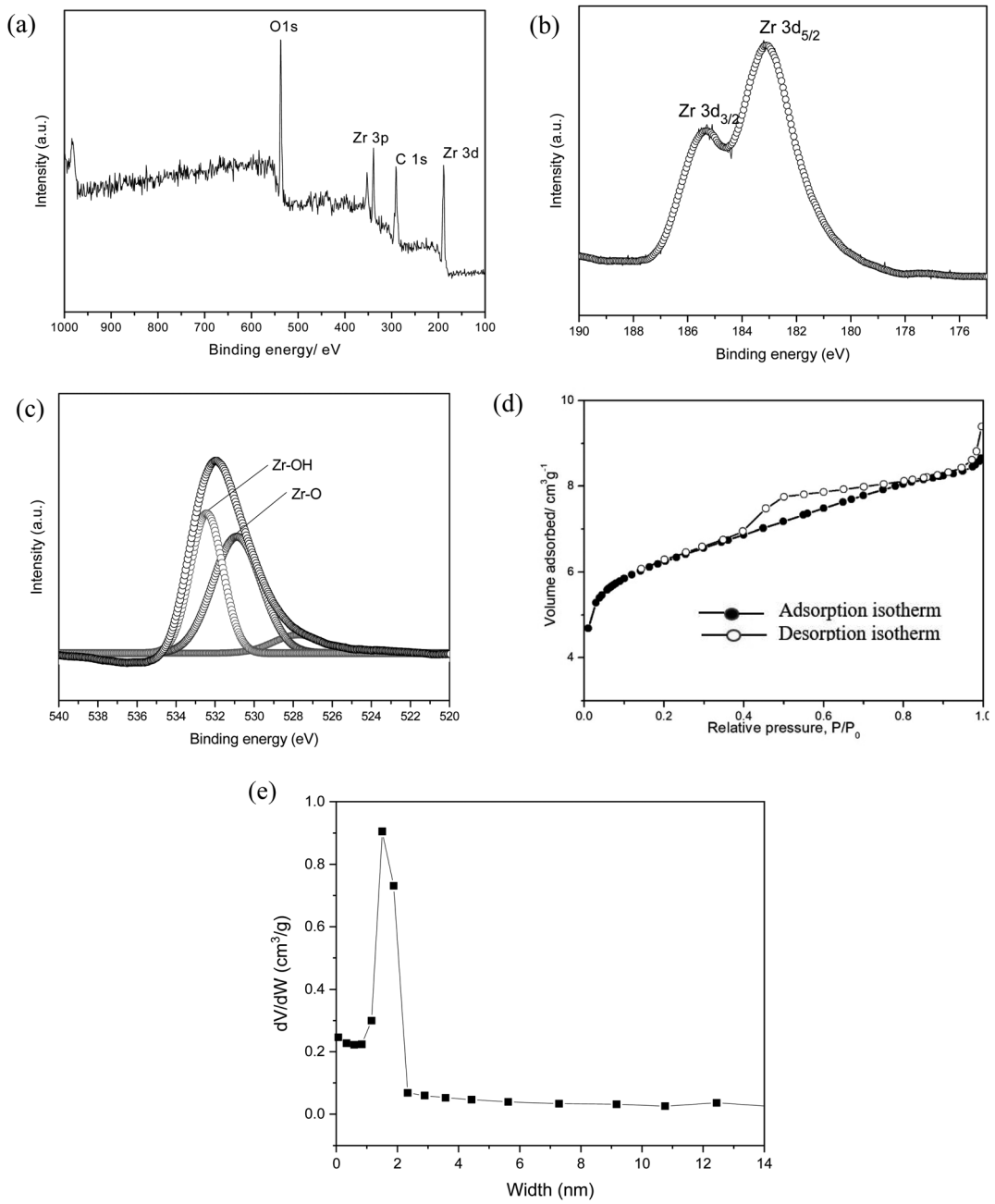

Fig. 3 (a) XPS wide scan of MOF-801, narrow scan of (b) Zr 3d, (c) O 1s, (d) the adsorption–desorption isotherm of N_2 in MOF-801 at 77 K and (e) pore size distribution of MOF-801.

adsorption process until equilibrium was achieved. Vivek Vardhan & Srimurali (2016) stated that equilibrium is achieved when the percentage of fluoride removed does not experience much improvement despite the longer contact time.[30] In this study, no considerable change in adsorption was observed after 120 min, so the reaction time for the supporting experiments was kept at 120 min.

3.2.2 Effect of amount of MOF-801. The dosage of the adsorbent is a vital parameter for determining the capacity of an adsorbent for a given initial concentration of the effluent. The effect of adsorbent dose on the fluoride removal efficiency (%) and adsorption capacity, q_e (mg g^{-1}) was studied using MOF-801 dose of 0.3, 0.6, 0.9, 1.2 and 1.5 g L^{-1}. In the meantime, the initial concentration of fluoride and contact time kept constant at 10 mg L^{-1} and 120 min respectively as shown in Fig. 4b. The percentage of fluoride removal increased from 54.5 to 95.2% with an increase in dosage of the MOF-801 adsorbent from 0.3 to 1.5 g L^{-1}. This result illustrated that the percent removal was increased with an increase in dosage of the adsorbent, because of an increase in the number of available active sites on the adsorbent surface until the adsorption achieved equilibrium. Equilibrium is achieved when the removal

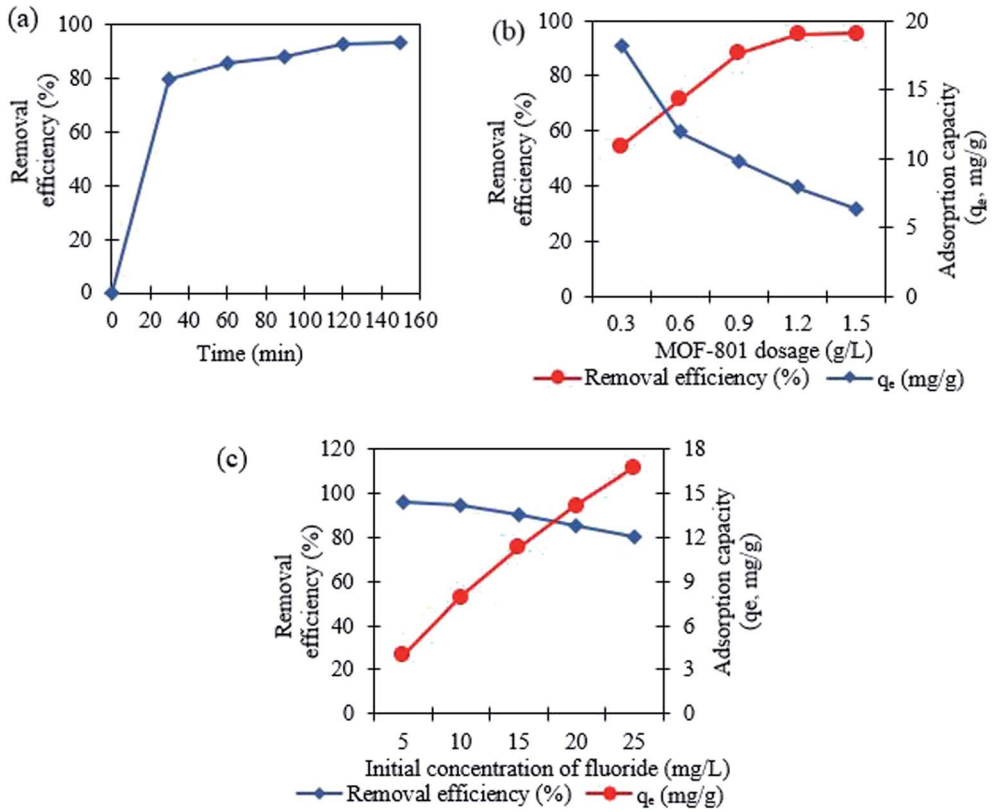

Fig. 4 (a) Effect of contact time on the fluoride adsorption by MOF-801, (b) effect of MOF-801 dosage and (c) effect of initial concentration of fluoride on the fluoride adsorption efficiency and adsorption capacity by MOF-801.

efficiency does not experience much increase despite an increase in the dose of adsorbent.[29] From Fig. 4b, it can be seen that the fluoride removal efficiency does not experience big increase after 0.9 g L^{-1}. Therefore, we further carried out the removal of fluoride at dosage of 1 g L^{-1} and the obtained removal percentage of fluoride was found to be 94.9% and this result showing that the adsorption had achieved its equilibrium at 1 g L^{-1}. Therefore, the optimum dose of MOF-801 for efficient removal of fluoride from water was found to be 1 g L^{-1}. Besides studying the percentage of fluoride removal by MOF-801, the adsorption capacity of MOF-801 was also studied since the capacity can reflect the properties of a material for removing fluoride ion from water. Adsorption capacity (q_e) refers to the amount of fluoride adsorbed per gram of MOF-801. Fig. 4b shows that the amount of fluoride adsorbed by MOF-801, decreased from 18.17 to 6.35 mg g^{-1} with an increase in dosage of the adsorbent from 0.3 to 1.5 g L^{-1}. This is because, as the dose of MOF-801 was increased, there were fewer fluoride ions per unit mass of MOF-801. In other words, the ratio of fluoride ions to MOF-801 decreased as the MOF-801 dosage increased.

3.2.3 Effect of initial concentration. The influence of initial concentration of fluoride ions on the adsorption of fluoride by MOF-801 was investigated, and the results are shown in Fig. 4c. The effect of initial fluoride concentration on the fluoride removal efficiency (%) was studied at fluoride concentrations of 5, 10, 15, 20 and 25 mg L^{-1} with the dose of MOF-801 and contact time kept constant at 1 g L^{-1} and 120 minutes respectively. It was observed that with an increase in fluoride ion concentration from 5–25 mg L^{-1}, there was an accompanying decrease in the percentage (%) removal of fluoride from 95.7 to 80.4%. This observation can be explained by considering the availability of adsorption sites. At low initial concentrations of fluoride ions, there would be more adsorption sites available. However, at higher concentrations, the presence of fluoride ions in the solution increases and most of the fluoride ions are left unabsorbed due to saturation of the adsorption sites. Since the dose of MOF-801 is limited at 1 g L^{-1}, the fluoride ions tend to compete for the active adsorption sites of MOF-801.[25,30] A standard isothermal graph of the amount of fluoride adsorbed onto MOF-801 at equilibrium (q_e) against equilibrium fluoride concentration in the solution (C_e) for initial fluoride concentrations from 5 to 25 mg L^{-1} is plotted as shown in Fig. 4c. The adsorption capacity increased linearly with the increase of the initial concentration of fluoride ions from 5–25 mg L^{-1}. The adsorption capacity of fluoride ion increased, and the removal efficiency decreased with the increasing initial concentrations of fluoride ions. This indicated that the increase of initial concentrations of fluoride ions contributed to enhance the driving force at the solid–liquid interface to increase the adsorption capacity until the exhaustion of active sites available for adsorption for fluoride. The obtained results proved that the adsorption efficacy was directly proportional to the initial concentration of fluoride ions. In order to describe the

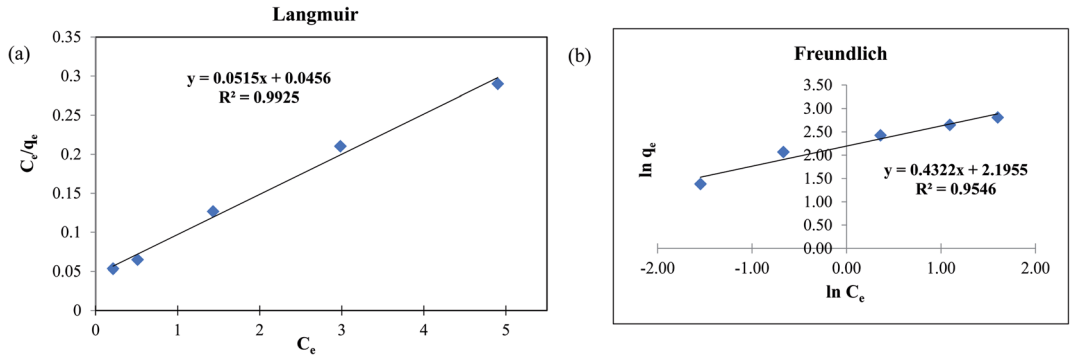

Fig. 5 Adsorption isothermal of MOF-801 as (a) Langmuir and (b) Freundlich isotherms for fluoride adsorption. Test conditions: adsorbent (1 g L^{-1}), reaction time (120 min) and fluoride solution (20 mL).

adsorption behaviours in detail, the experimental data were then fitted with the Freundlich and Langmuir isotherm models in Section 3.3.

3.3 Adsorption isotherm studies

The adsorption isotherm is used to describe the steadiness of adsorption process in liquid–solid system. The fluoride adsorption isotherms were investigated using the data collected for the effect of initial concentration of 5 to 25 mg L^{-1} of fluoride solution as discussed in the previous Section 3.2.3. It is clear that the adsorption capacity increases with the increasing fluoride concentration. Here, to explain the connection among adsorbate and adsorbent using MOF-801, Langmuir and Freundlich isotherm model were used. Fig. 5a and b shows the Langmuir and Freundlich isotherm models fitted to the experimental data plotted using the eqn (5) and (6) respectively. The experimental data used for both Langmuir and Freundlich isothermal models are for 1 g L^{-1} dose of MOF-801 in 20 mL of different initial concentrations of fluoride in the solution.

3.3.1 Langmuir isotherm. The Langmuir model is one of the prominent models which assumes that adsorption leads to a monolayer formation without interaction between the adsorbate molecules with all the adsorption sites of the solid surface. This model is focused on the idea that no development of strong bonds is possible on the surface of the adsorbate where all the specific sites onto adsorbent surface has constant binding energy.[31,32] The calculated parameters from the fitting curves are summarised in Table 1. From the Langmuir isotherm model in Fig. 5a, the equation obtained for the straight line is $y = 0.0515x + 0.0456$. The gradient and y-intercept obtained from the graph were used to calculate maximum adsorption capacity (q_m) and Langmuir constant (K_L).

3.3.2 Freundlich isotherm. The Freundlich isotherm model is based on the adsorbate arrives at the non-uniform surface of the adsorbent with different adsorption sites having different adsorption energies, was also known as uneven multilayer adsorption.[33] From Fig. 5b, the linear equation for Freundlich isotherm model obtained to be $y = 0.04322x + 2.1955$. The gradient and y-intercept obtained from the graph were used to calculate relative adsorption capacity (K_F) and intensity of adsorption (n).

Table 1 compares the Langmuir and Freundlich isothermal constants for the adsorption of fluoride onto MOF-801. The linear correlation coefficient R^2 of the Langmuir isotherm model was 0.9925 whereas the corresponding value for the proposed Freundlich isotherm model was 0.9546. The values suggest that the best fitting isothermal model for adsorption of fluoride on MOF-801 is the Langmuir model, based on its closeness of R^2 value to 1 and consequently the adsorption process occurs homogeneously in a monolayer manner. Moreover, the calculated q_m obtained was 19.42 mg g^{-1} and the Langmuir constant was found to be 1.129 L g^{-1}. The q_m of 19.42 mg g^{-1} reported in this study is higher than that of few other adsorbents in literature such as hydrous ferric oxide (16.5 mg g^{-1}),[34] chitosan composite (1.25 mg g^{-1})[35] and granular ceramic (12.12 mg g^{-1}).[11]

Based on the Langmuir isotherm model, the adsorption of fluoride on MOF-801 is likely to occur *via* chemisorption due to the monolayer formation.[31,36] MOF-801 is assumed to have homogeneous surface-active sites which are all identical and energetically equivalent. The Langmuir separation factor R_L was calculated to further explain the favourability of fluoride adsorption on MOF-801. The equation to calculate R_L is shown in eqn (7).

Table 1 Comparison of isothermal constants for adsorption of fluoride

Isotherm model	Langmuir	Freundlich
Isotherm parameters	q_m (mg g^{-1}) = 19.42 K_L (L mg^{-1}) = 1.1292 R^2 = 0.9925	K_F (mg g^{-1}) (L mg^{-1})$^{1/n}$ = 8.984 n = 2.3137 R^2 = 0.9546

Table 2 The nature of adsorption process based on R_L value[34]

R_L Value	Nature of adsorption process
$R_L = 0$	Irreversible
$0 < R_L < 1$	Favourable
$R_L = 1$	Linear
$R_L > 1$	Unfavourable

$$R_L = 1/(1 + K_L C_0) \quad (7)$$

where C_0 is the initial concentration of fluoride, K_L is the Langmuir isotherm constant and R_L is the dimensionless constant separation factor of Langmuir isotherm. The R_L for adsorption of fluoride on MOF-801 was found to be 0.0824. Since the R_L is in between 0 to 1, the adsorption of fluoride on MOF-801 is a favourable process. The nature of adsorption process using the Langmuir model for different R_L value is shown in Table 2.

3.4 Adsorption kinetics studies

To establish the adsorption kinetics and the adsorption equilibrium time, the adsorption of fluoride by MOF-801 was investigated as a function of contact time. To determine the rate of fluoride adsorption on MOF-801, the commonly used adsorption kinetic models of the pseudo-first-order and pseudo-second-order were applied to determine the related adsorption kinetics parameter. Pseudo-first-order model is followed by adsorption reaction preceded by diffusion through a boundary whereas pseudo-second-order model is commonly followed by adsorption process with chemisorption being the rate-control.[27] Khayyun (2019) suggested that the adsorption model which best fits the experimental data has the ability to explain the adsorption better.[37] Fig. 6a and b show the fitting plots of pseudo-first-order and pseudo-second-order model. The linear equation obtained from the plot of pseudo-first-order model in Fig. 6a is $y = -0.0168x + 1.2782$. On the other hand, the linear equation obtained from the pseudo-second order plot is $y = 0.0611x + 0.4994$. The gradient and y-intercept obtained from the linear equation is used to calculate k_1 or k_2, $q_{e,cal}$ respectively.

The corresponding adsorption kinetics model parameter of fluoride adsorbed on MOF-801 is shown in Table 3. The pseudo-second-order model fits better for the fluoride adsorption according to the relatively higher correlation coefficient ($R^2 = 0.9991$) compared with the pseudo-first-order model ($R^2 = 0.9477$). Furthermore, the calculated adsorption amounts of pseudo-second-order model ($q_{e,cal} = 16.37$ mg g^{-1}) agree well with the experimental values ($q_{e,expt} = 15.59$ mg g^{-1}) compared to the calculated adsorption amounts of pseudo-first-order model ($q_{e,cal} = 3.59$ mg g^{-1}) which was not close to the value of experimental adsorption capacity. Therefore, the adsorption of fluoride on MOF-801 can be described well with the pseudo-second-order model instead of pseudo-first-order model, which is based on the assumption that the rate-limiting step should be mainly chemisorption involving covalent bonds *via* sharing or exchange of electrons between anion and adsorbent. This study reported the higher $q_{e,cal}$ (16.37 mg g^{-1}) and $q_{e,expt}$ (15.59 mg g^{-1}) of the solvothermal synthesized MOF-801 than of hydrothermally synthesized MOF-801 ($q_{e,cal} = 13.70$ mg g^{-1} and $q_{e,expt} = 13.59$ mg g^{-1}) reported by[24] for the removal of fluoride from water.

Table 3 Kinetic parameters for fluoride adsorption on MOF-801

Experimental data		Pseudo-first-order		Pseudo-second-order	
$q_{e,expt}$ (mg g^{-1})	15.59	$q_{e,cal}$ (mg g^{-1})	3.590	$q_{e,cal}$ (mg g^{-1})	16.37
		k_1 (min^{-1})	0.039	k_2 (min^{-1})	0.0075
		R^2	0.9477	R^2	0.9991

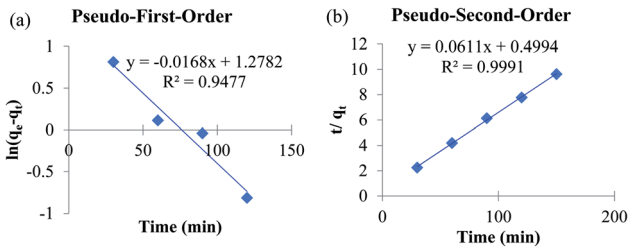

Fig. 6 Adsorption kinetics of MOF-801 as (a) pseudo-first-order and (b) pseudo-second-order for fluoride adsorption. Test conditions: adsorbent (1 g L^{-1}) and fluoride solution (20 mL).

3.5 Adsorption mechanism

The properties and structure of MOF-801, especially high surface area and micro porosity make them highly efficient at removing fluoride from water. The adsorption process of MOF-801 for fluoride removal follows Langmuir isotherm model with pseudo-second order fitting. Based on the adsorption isotherm and kinetics results discussed above, the mechanism for depicting the fluoride adsorption process onto MOF-801 is suggested to be chemisorption due to the monolayer formation. The chemisorption mechanism for fluoride removal by MOF-801 is most likely due to ion exchange of fluoride ions and hydroxyl groups within the adsorbent.[24] The hydroxyl groups on the metal-nodes within the structure of MOF-801 is substituted by fluoride ions *via* the anion exchange behaviour.[38] Anion exchange behaviour refers to any ions with negatively charged ions that can be exchanged stoichiometrically with similarly charged ions in the aqueous phase of a chemical process.[39] The unique anion-exchange mechanism of MOF-801 can be attributed to the isoelectronic and comparable ionic radii between hydroxyl and fluoride ion, and by the electrostatic interaction between zirconium cation and fluoride ion as shown in eqn (8) below.

$$Zr\text{–}OH + F^- \rightarrow Zr\text{–}F + OH^- \quad (8)$$

The highly specificity of MOF-801 towards fluoride ions is due to the relatively greater electronegativity and higher electron withdrawing property of fluorine compared to oxygen and others halogen elements, which renders the substitution of

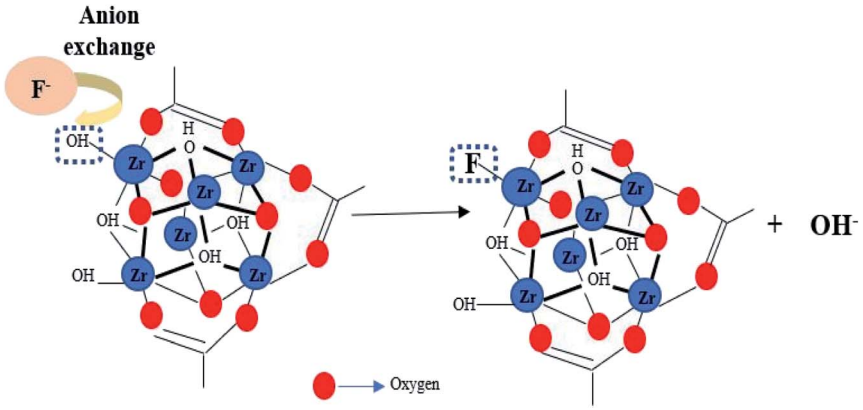

Fig. 7 Proposed mechanism of MOF-801 for fluoride adsorption.

hydroxyl ions by fluoride ions to be energetically favourable on MOF-801. Furthermore, the unique octahedral nature of the zirconium centre increases accessibility of the exchange site and improves diffusion throughout the framework, which leads to the effective removal of fluoride ions. Moreover, the adsorption affinity towards fluoride ion could also be applied to other types of metal-based MOF such as hafnium (Hf) based MOF, which is gaining popularity. This is because Hf chemically resembles zirconium in terms of both structure, charge (Hf^{4+} and Zr^{4+}) and properties. The proposed mechanism for fluoride removal by MOF-801 was shown in Fig. 7.

3.6 Regeneration studies of MOF-801

Regeneration studies refer to the reusability of the adsorbent, which in turn reduce operational cost and protect the environment. The regeneration treatment can be done using salts, acids, or bases. Various studies have shown that the use of strong acid (*e.g.* HCl) or base (*e.g.* NaOH) for regenerating the adsorbent could result in relatively high fluoride removal efficiencies.[40–42] However, HCl treatment could cause the leaching of the Zr component and damage the adsorbent. NaOH is found to favour the replacement of OH^- with F^- and was found to be the most effective solution for regeneration of MOF-801.

The efficiency of porous MOF-801 is evaluated for their repeated regeneration for fluoride ion removal experiments using 0.1 M NaOH (20 mL). After an adsorption cycle, MOF-801 becomes exhausted and saturated with fluoride ions. The fluoride saturated MOF-801 was then defluorinated and regenerated to be reused for the next adsorption cycle. The percentage of fluoride removed from the first cycle to the fourth cycle were 91.8%, 87.7%, 84.6% and 78.9% respectively as shown in Fig. 8a. The obtained results show that the adsorption efficacy of porous MOF-801 for fluoride ion adsorption gradually decreases with repeated use of MOF-801. According to Vivek Vardhan & Srimurali (2016), the decrease in the fluoride removal efficiency of an adsorbent after each regeneration cycle may be attributed to the chemisorption of previously adsorbed fluoride which was not removed completely from the adsorbent during the desorption process.[30] There is a strong chemical bonding interaction between the MOF-801 and the fluoride during the chemisorption process, which makes the

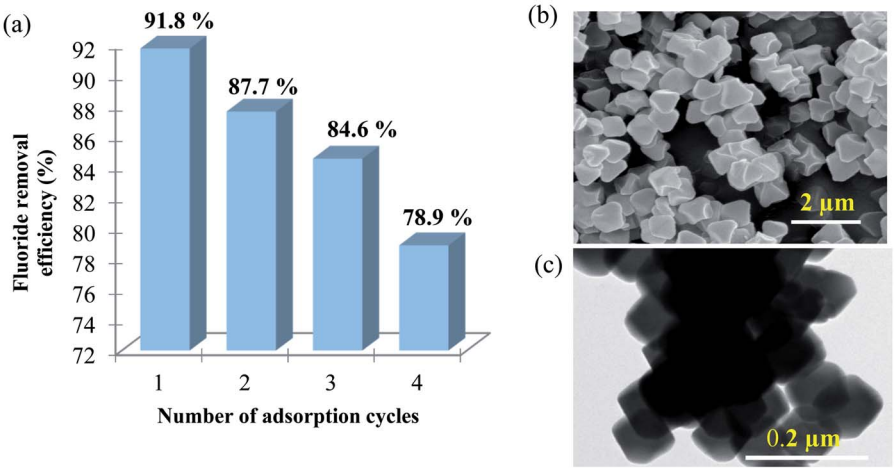

Fig. 8 (a) Fluoride removal efficiency (%) for regenerated MOF-801 for each adsorption cycle, (b) SEM and (c) TEM image of MOF-801 after 4th fluoride adsorption.

Table 4 Comparison of the removal efficiencies (%) of fluoride of regenerated MOF-801 with other regenerated adsorbents in literature

Types of adsorbent	Cycle 1 (%)	Cycle 2 (%)	Cycle 3 (%)	Cycle 4 (%)	References
MOF-801	91.80	87.70	84.60	78.90	Present work
Lanthanum-impregnated bauxite	95.00	94.00	93.00	92.00	30
Zr-MOF	92.90	91.20	89.90	88.90	44
Bauxite	94.00	—	—	—	45
Bone char	92.45	—	—	—	46

regeneration process difficult and thus, decreases the reusability of the adsorbent. Fig. 8b and c show that the octahedral shaped morphology of MOF-801 is retained after the four times repeated utilization of MOF-801 for fluoride adsorption, indicating relatively good stability of MOF-801 in the regeneration process.

The fluoride removal efficiency of the regenerated MOF-801 in this present work was compared with other adsorbents in literature as shown in Table 4. Table 4 shows that the removal efficiency exhibited by MOF-801 was quite close and within range of the removal efficiency of the other reported adsorbents such as zirconium, lanthanum-impregnated bauxite, bone char and bauxite. The slightly lower value of removal efficiency obtained in this study compared to the other adsorbents was due to the lower concentration of NaOH used to regenerate MOF-801. In this study, only 0.1 M (or 0.2%) of NaOH was used to regenerate MOF-801 whereas for other reported studies such as zirconium metal–organic frameworks (Zr-MOFs), lanthanum-impregnated bauxite and bone char reported in Table 4 were regenerated using NaOH of 3% 4% and 2% respectively. A lower concentration of NaOH was used to regenerate MOF-801 because higher concentrations of NaOH can cause modifications of the adsorbent structure.[43] Interestingly, it has to be noted that, MOF-801 was able to exhibit comparable removal efficiency despite the lower concentration of NaOH used. MOF-801 can be reused due to the micrometre-sized structure with high surface area, which is important in reducing the overall cost for adsorption process in practical applications.

4. Conclusions

In summary, MOF-801 was prepared by a simple solvothermal method and MOF-801 has exhibited excellent performance in the adsorption of fluoride from water. The morphology, porous structure and their adsorption performance for fluoride was systematically investigated. The prepared MOF-801 with high surface area of 522 $m^2 g^{-1}$ has an optimum adsorption amount for fluoride of up to 17.33 mg g^{-1}. The effect of various process parameters showed that the adsorption percentage increased with increase in contact time and adsorbent dose, whereas there was a decrease in adsorption percentage of fluoride ion with increase in fluoride initial concentration. MOF-801 showed rapid adsorption kinetics at the initial stages of adsorption, which became slower upon reaching equilibrium. The kinetic studies showed that the adsorption of fluoride follows the Langmuir isotherm model and could be fitted-well with a pseudo-second-order model, thus deducing that the fluoride adsorption behaviour of MOF-801 is based on chemisorption. The regeneration studies of MOF-801 indicated that MOF-801 was able to be reused up to four cycles for the adsorption of fluoride ion. The results of this study suggests that an adsorption system utilizing MOF-801 would demonstrate a good capacity for fluoride adsorption, highlighting its potential as an effective adsorbent for the treatment of fuoride from aqueous solution.

Conflicts of interest

There are no conflicts to declare.

Acknowledgements

The authors gratefully acknowledge the support from Institute of Advanced Technology, Universiti Putra Malaysia and Synchrotron Light Research Institute (SLRI), Thailand for material characterizations.

References

1 Q. Song, Y. Fang, J. Wang, J. Liang, Q. Hu, Z. Liu, *et al.*, Enhanced adsorption of fluoride on Al-modified boron nitride nanosheets from aqueous solution, *J. Alloys Compd.*, 2019, **793**, 512–518.
2 World Health Organization, *Guidelines for Drinking-water Quality*, World Health Organization, 2011, 4th edn, pp. 1–541.
3 H. M. Herath, T. Kawakami and M. Tafu, The extremely high adsorption capacity of fluoride by chicken bone char (CBC) in defluoridation of drinking water in relation to its finer particle size for better human health, *Healthcare*, 2018, **6**(4), 123.
4 Y. Xia, X. Huang, W. Li, Y. Zhang and Z. Li, Facile defluoridation of drinking water by forming shell@ fluorapatite nanoarray during boiling eggshell, *J. Hazard. Mater.*, 2019, **361**, 321–328.
5 S. Chatterjee, M. Mukherjee and S. De, Groundwater defluoridation and disinfection using carbonized bone meal impregnated polysulfone mixed matrix hollow-fiber membranes, *J. Water Process Eng.*, 2020, **33**, 101002.
6 X. Wang, S. Pan, M. Zhang, J. Qi, X. Sun, C. Gu, *et al.*, Modified hydrous zirconium oxide/PAN nanofibers for efficient defluoridation from groundwater, *Sci. Total Environ.*, 2019, **685**, 401–409.

7 Y. Zhang, L. Xiong, Y. Xiu and K. Huang, Defluoridation in fixed bed column filled with Zr (IV)-loaded garlic peel, *Microchem. J.*, 2019, **145**, 476–485.
8 M. Amini, K. Mueller, K. C. Abbaspour, T. Rosenberg, M. Afyuni, K. N. Møller, M. Sarr, *et al.*, Statistical modeling of global geogenic fluoride contamination in groundwaters, *Environ. Sci. Technol.*, 2008, **42**(10), 3662–3668.
9 E. Kowalchuk, *Selective fluoride removal by aluminum precipitation & membrane filtration*, 2012.
10 R. Araga, S. Soni and C. S. Sharma, Fluoride adsorption from aqueous solution using activated carbon obtained from KOH-treated jamun (Syzygium cumini) seed, *J. Environ. Chem. Eng.*, 2017, **5**(6), 5608–5616.
11 N. Chen, Z. Zhang, C. Feng, N. Sugiura, M. Li and R. Chen, Fluoride removal from water by granular ceramic adsorption, *J. Colloid Interface Sci.*, 2010, **348**(2), 579–584.
12 S. Ayoob, A. K. Gupta and V. T. Bhat, A conceptual overview on sustainable technologies for the defluoridation of drinking water, *Crit. Rev. Environ. Sci. Technol.*, 2008, **38**(6), 401–470.
13 C. A. Babu, D. Sujish, M. S. Murugappa, G. Mohanakrishnan, P. Kalyanasundaram and B. Raj, A comprehensive treatment method for defluoridation of drinking water, *Indian J. Chem. Technol.*, 2011, **18**(4), 314–318.
14 H. Furukawa, K. E. Cordova, M. O'Keeffe and O. M. Yaghi, The chemistry and applications of metal-organic frameworks, *Science*, 2013, **341**(6149), 1230444.
15 S. Rajkumar, S. Murugesh, V. Sivasankar, A. Darchen, T. A. Msagati and T. Chaabane, Low-cost fluoride adsorbents prepared from a renewable biowaste: syntheses, characterization and modeling studies, *Arabian J. Chem.*, 2019, **12**(8), 3004–3017.
16 A. Salifu, *Fluoride Removal from Groundwater by Adsorption Technology*, CRC Press, 2017.
17 M. Mohapatra, S. Anand, B. K. Mishra, D. E. Giles and P. Singh, Review of fluoride removal from drinking water, *J. Environ. Manage.*, 2009, **91**(1), 67–77.
18 J. M. Yang, X. W. Hu, Y. X. Liu and W. Zhang, Fabrication of a carbon quantum dots-immobilized zirconium-based metal-organic framework composite fluorescence sensor for highly sensitive detection of 4-nitrophenol, *Microporous Mesoporous Mater.*, 2019, **274**, 149–154.
19 G. Yuan, H. Tu, M. Li, J. Liu, C. Zhao, J. Liao, *et al.*, Glycine derivative-functionalized metal-organic framework (MOF) materials for Co (II) removal from aqueous solution, *Appl. Surf. Sci.*, 2019, **466**, 903–910.
20 W. Yu, M. Luo, Y. Yang, H. Wu, W. Huang, K. Zeng, *et al.*, Metal-organic framework (MOF) showing both ultrahigh As (V) and As (III) removal from aqueous solution, *J. Solid State Chem.*, 2019, **269**, 264–270.
21 C. Chen, D. Chen, S. Xie, H. Quan, X. Luo and L. Guo, Adsorption behaviors of organic micropollutants on zirconium metal–organic framework UiO-66: analysis of surface interactions, *ACS Appl. Mater. Interfaces*, 2017, **9**(46), 41043–41054.
22 D. T. Nguyen, H. T. Le, T. S. Do, V. T. Pham, L. Dai Tran, V. T. Ho, *et al.*, Metal-organic framework MIL-53 (Fe) as an adsorbent for ibuprofen drug removal from aqueous solutions: response surface modelling and optimization, *J. Chem.*, 2019, **2019**, 1–11.
23 S. Chen, F. Feng, S. Li, X. X. Li and L. Shu, Metal-organic framework DUT-67 (Zr) for adsorptive removal of trace Hg^{2+} and CH_3Hg^+ in water, *Chem. Speciation Bioavailability*, 2018, **30**(1), 99–106.
24 X. H. Zhu, C. X. Yang and X. P. Yan, Metal-organic framework-801 for efficient removal of fluoride from water, *Microporous Mesoporous Mater.*, 2018, **259**, 163–170.
25 F. Ke, C. Peng, T. Zhang, M. Zhang, C. Zhou, H. Cai, *et al.*, Fumarate-based metal-organic frameworks as a new platform for highly selective removal of fluoride from brick tea, *Sci. Rep.*, 2018, **8**(1), 1–11.
26 M. Taddei, M. J. McPherson, A. Gougsa, J. Lam, J. Sewell and E. Andreoli, An Optimised Compaction Process for Zr-Fumarate (MOF-801), *Inorganics*, 2019, **7**(9), 110.
27 J. He, X. Cai, K. Chen, Y. Li, K. Zhang, Z. Jin, *et al.*, Performance of a novelty-defined zirconium metal-organic frameworks adsorption membrane in fluoride removal, *J. Colloid Interface Sci.*, 2016, **484**, 162–172.
28 L. Liu, Z. Qiao, X. Cui, C. Pang, H. Liang, P. Xie, *et al.*, Amino Acid Imprinted UiO-66s for Highly Recognized Adsorption of Small Angiotensin-Converting-Enzyme-Inhibitory Peptides, *ACS Appl. Mater. Interfaces*, 2019, **11**(26), 23039–23049.
29 A. Goswami, Treatment Of Fluoride Containing Water Using Adsorption And Precipitation Followed By Microfiltration, Doctoral dissertation, Indian Institute of Technology Guwahati, 2013.
30 C. V. Vardhan and M. Srimurali, Removal of fluoride from water using a novel sorbent lanthanum-impregnated bauxite, *SpringerPlus*, 2016, **5**(1), 1426.
31 E. I. Unuabonah, K. O. Adebowale, B. I. Olu-Owolabi, L. Z. Yang and L. Kong, Adsorption of Pb (II) and Cd (II) from aqueous solutions onto sodium tetraborate-modified kaolinite clay: equilibrium and thermodynamic studies, *Hydrometallurgy*, 2008, **93**(1–2), 1–9.
32 R. E. Treybal, *Mass transfer operations*, New York, 1980, p. 466.
33 R. S. Juang, F. C. Wu and R. L. Tseng, The ability of activated clay for the adsorption of dyes from aqueous solutions, *Environ. Technol.*, 1997, **18**(5), 525–531.
34 S. Dey, S. Goswami and U. C. Ghosh, Hydrous ferric oxide (HFO)—a scavenger for fluoride from contaminated water, *Water, Air, Soil Pollut.*, 2004, **158**(1), 311–323.
35 N. Viswanathan and S. Meenakshi, Selective fluoride adsorption by a hydrotalcite/chitosan composite, *Appl. Clay Sci.*, 2010, **48**(4), 607–611.
36 G. H. Safari, M. Zarrabi, M. Hoseini, H. Kamani, J. Jaafari and A. H. Mahvi, Trends of natural and acid-engineered pumice onto phosphorus ions in aquatic environment: adsorbent preparation, characterization, and kinetic and equilibrium modeling, *Desalin. Water Treat.*, 2015, **54**(11), 3031–3043.

37 T. S. Khayyun and A. H. Mseer, Comparison of the experimental results with the Langmuir and Freundlich models for copper removal on limestone adsorbent, *Appl. Water Sci.*, 2019, **9**(8), 170.
38 M. J. Slater, *Principles of ion exchange technology*, Butterworth-Heinemann, 2013.
39 P. Wu, J. Wu, L. Xia, Y. Liu, L. Xu and S. Song, Adsorption of fluoride at the interface of water with calcined magnesium–ferri–lanthanum hydrotalcite-like compound, *RSC Adv.*, 2017, **7**(42), 26104–26112.
40 A. K. Kanyora, T. K. Kinyanjui, S. M. Kariuki and C. K. Chepkwony, Efficiency of various sodium solutions in regeneration of fluoride saturated bone char for de-fluoridation, *IOSR J. Environ. Sci., Toxicol. Food Technol.*, 2014, **8**, 10–16.
41 J. Zhang, Y. Kong, Y. Yang, N. Chen, C. Feng, X. Huang, *et al.*, Fast Capture of Fluoride by Anion-Exchange Zirconium–Graphene Hybrid Adsorbent, *Langmuir*, 2019, **35**(21), 6861–6869.
42 A. Rafique, M. A. Awan, A. Wasti, I. A. Qazi and M. Arshad, Removal of fluoride from drinking water using modified immobilized activated alumina, *J. Chem.*, 2012, **2013**, 1–7.
43 T. Nur, P. Loganathan, T. C. Nguyen, S. Vigneswaran, G. Singh and J. Kandasamy, Batch and column adsorption and desorption of fluoride using hydrous ferric oxide: solution chemistry and modeling, *Chem. Eng. J.*, 2014, **247**, 93–102.
44 J. He, X. Cai, K. Chen, Y. Li, K. Zhang, Z. Jin, *et al.*, Performance of a novelly-defined zirconium metal-organic frameworks adsorption membrane in fluoride removal, *J. Colloid Interface Sci.*, 2016, **484**, 162–172.
45 N. M. Ippolito, G. Maffei, F. Medici and L. Piga, Adsorption and regeneration of fluoride ion on a high alumina content bauxite, *Chem. Eng. Trans.*, 2016, **47**, 217–222.
46 A. Kanyora, T. Kinyanjui, S. Kariuki and M. Njogu, Fluoride removal capacity of regenerated bone char in treatment of drinking water, *Asian Journal of Natural and Applied Sciences*, 2015, **4**, 1.